Preclinical efficacy and safety of adeno-associated virus 5 alpha-galactosidase: A gene therapy for Fabry disease

Jolanda M.P. Liefhebber,[1] Giso Brasser,[1] Elisabeth A. Spronck,[1] Roelof Ottenhoff,[2] Lieke Paerels,[1] Maria J. Ferraz,[3] Lukas K. Schwarz,[1] Nikoleta Efthymiopoulou,[1] Chi-Lin Kuo,[3,4] Paula S. Montenegro-Miranda,[1,5] Melvin M. Evers,[1] Johannes M.F.G. Aerts,[3] and Ying Poi Liu[1]

[1]uniQure biopharma B.V., Amsterdam 1105 BP, the Netherlands; [2]Amsterdam UMC, Amsterdam 1105 AZ, the Netherlands; [3]Leiden Institute of Chemistry, Leiden University, Leiden 2333 CC, the Netherlands; [4]VIB, 9052 Ghent, Belgium; [5]VectorY Therapeutics B.V., Amsterdam 1098 XH, the Netherlands

We developed a novel adeno-associated virus 5 gene therapy (AAV5-GLA) expressing human alpha-galactosidase A (GLA) under the control of a novel, small and strong, liver-restricted promoter. We assessed the preclinical potential of AAV5-GLA for treating Fabry disease, an X-linked hereditary metabolic disorder resulting from mutations in the gene encoding GLA that lead to accumulation of the substrates globotriaosylceramide and globotriaosylsphingosine, causing heart, kidney, and central nervous system dysfunction. Effects of intravenously administered AAV5-GLA were evaluated in (1) GLA-knockout mice aged 7–8 weeks (early in disease) and 20 weeks (nociception phenotype manifestation) and (2) cynomolgus macaques during an 8-week period. In both species, AAV5-GLA was observed as safe, generated detectable vector DNA and mRNA levels in liver, and produced stable enzyme activity in liver and plasma. In mice, dose-dependent transgene enzyme activity, cross-correction (substrate reduction) in kidney and heart, and improved nociception lasted over 6 months. Moreover, after delayed administration when animals displayed the nociception phenotype, target organ enzyme activity was present, and accumulated substrates were reduced. Given the strong, durable expression of active GLA with this promoter and favorable profile of adeno-associated virus 5-based gene therapy in humans, AAV5-GLA warrants further investigation in clinical trials for Fabry disease.

INTRODUCTION

Adeno-associated virus (AAV) vector gene delivery systems have shown success in human gene-therapy applications, with several now approved for clinical use.[1–3] We have developed an AAV5 vector-based gene therapy expressing human alpha-galactosidase A (GLA) under the control of a novel, small and strong, liver-restricted proprietary promoter (AAV5-GLA). This investigational gene therapy uses the validated AAV5 technology of HEMGENIX (etranacogene dezaparvovec-drlb), a liver-directed gene therapy for hemophilia B. AAV5-GLA was developed to be a potential one-time treatment for Fabry disease, which is a rare, inherited, multi-systemic, X-linked, lysosomal storage disorder.[4,5]

Fabry disease is caused by pathogenic loss-of-function mutations in the gene encoding the lysosomal enzyme GLA, resulting in absent or markedly deficient GLA activity.[4,6] Because GLA is required for the breakdown of globotriaosylceramide (Gb3) and its deacylated form, globotriaosylsphingosine (lyso-Gb3), in patients with Fabry disease, these glycosphingolipids accumulate within lysosomes, which leads to progressive pathology in multiple tissues and organ systems,[6] particularly the cardiovascular, renal, and nervous systems.[4,7] Patients have a shortened lifespan and experience complications such as renal failure, cardiac disease, acroparesthesias (neuropathic pain in hands and feet), gastrointestinal symptoms, and stroke.[8,9]

The current standard of care for Fabry disease is GLA enzyme replacement therapy (ERT) using recombinant GLA, which slows the progression of heart and kidney disease.[10] Furthermore, ERT requires individuals to undergo lifetime intravenous infusions every 2 weeks and is characterized by a short plasma half-life that results in peaks and troughs of the recombinant enzyme that limit its tissue distribution.[11] Unless initiated early in the disease course, ERT has a limited effect on the cardiac manifestations of disease.[6] Thus, improved treatments are needed for Fabry disease.

AAV5-GLA gene therapy has been designed to provide long-term replacement of GLA activity in patients with Fabry disease after a single infusion via liver-specific GLA expression that is driven from a novel, small and strong, liver-restricted, proprietary promoter. Durable transgene expression has been demonstrated with a similarly structured AAV5-based gene therapy expressing human factor IX in adults with hemophilia B.[12,13] To further decrease the risk of potential immune responses against a foreign transgene, we limited the location of its expression using a liver-restricted promoter, a strategy previously shown to be beneficial for durable expression and that may induce
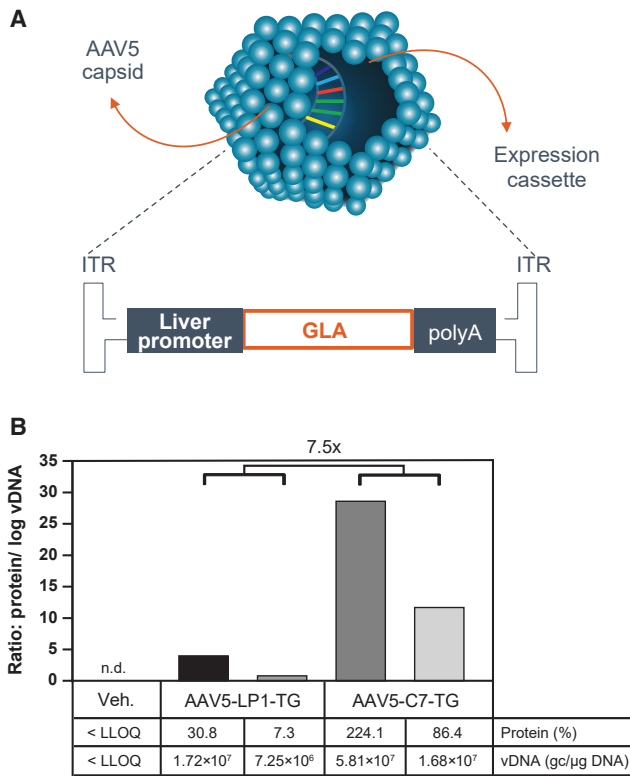
Figure 1. Development of a novel, small and strong, liver-specific promoter for Fabry disease gene therapy

(A) AAV5 capsid-based vector containing a liver-restricted proprietary promoter, cDNA of human GLA enzyme (in the case of AAV5-GLA vector), an SV40 poly(A) signal sequence, and flanking ITRs. (B) Vector, containing either the LP1 or C7 promoter in front of the cDNA of an unrelated TG, was administered at similar doses to cynomolgus monkeys ($n = 2$). Liver vDNA (gc/μg DNA) was measured at 16 weeks post infusion, and data per individual monkey were averaged over eight sections. Levels of a transgene protein (unrelated to GLA) were measured in plasma, and results are shown as the average from multiple measurements taken during the 4- to 16-week time period (as % of normal human plasma levels). The ratios between transgene protein and log vDNA levels were plotted. AAV5, adeno-associated virus 5; GLA, alpha-galactosidase A; ITR, inverted terminal repeat; LLOQ, lower limit of quantification; n.d., not determined; polyA, polyadenylated tail; TG, transgene; vDNA, vector DNA.

immune tolerance.[14–18] The objective of the preclinical studies described here was to assess the efficacy and safety of AAV5-GLA gene therapy in (1) a mouse model of Fabry disease and (2) non-human primates (NHPs) as a potential therapeutic option for patients.

RESULTS

Liver promoter comparison

To test our novel, liver-restricted (C7) promoter, we compared it *in vivo* with the LP1 promoter previously developed by Nathwani et al.[19] Intravenous infusion of cynomolgus monkeys with both AAV5 vectors (C7 and LP1) resulted in detectable production of an unrelated transgene protein in plasma (Figure 1), indicating that the vectors could be transduced into the NHP liver to express an active transgene product. Our

optimized, novel, small and strong, liver-restricted proprietary promoter produced, on average, a 7.5-fold increase in transgene protein levels compared with those produced with the vector containing the LP1 liver promoter. Liver specificity of the C7 promoter was observed, because, in most organs, mRNA levels were below the lower limit of quantification (LLOQ) of the reverse transcription quantitative polymerase chain reaction (RT-qPCR) assay (data not shown, but confirmed in Figure 3). For the liver, the ratio of transgene mRNA to vector DNA (vDNA) was close to 1:50. In contrast, for the adrenal gland, the only other organ with mRNA levels above the LLOQ, this ratio was much smaller, at 1:2,500. Peripheral organs including the spleen, heart, and kidney had more than 1×10^6 genome copies (gc)/μg vDNA but had mRNA levels below the LLOQ (4×10^3 copies/μg RNA); therefore, the calculated ratio mRNA:vDNA was less than 1:250, indicating liver specificity of the C7 promoter. We continued development of an AAV5 gene therapy with the novel, small and strong, liver-restricted proprietary C7 promoter for Fabry disease.

AAV5-GLA liver transduction and transgene expression

For Fabry disease, an AAV5 vector was developed for the expression of human GLA as a transgene under the control of the novel C7 promoter (AAV5-GLA). To further investigate the preclinical potential of AAV5-GLA, the vector was administered intravenously to mice and NHPs. As a model for Fabry disease, the GLA-knockout (GLA-KO) mouse was used.[20] The knockout abolishes GLA gene expression and results in a continuous buildup of substrates, leading to highly increased levels of Gb3 and lyso-Gb3, as observed in patients with Fabry disease.[21] AAV5-GLA effectively transduced the liver of both GLA-KO mice and NHPs, as shown by detectable vDNA and GLA mRNA in the liver of treated animals (Figure 2). Experiments in GLA-KO mice showed a dose-response effect on vDNA content and mRNA production (Figure 2A). Mouse livers were stained by fluorescence *in situ* hybridization (FISH) using a probe against human GLA recognizing both vDNA and transgene mRNA. A semi-quantitative analysis demonstrated a dose-response effect on the percentage of cells positive for the FISH probe, with a maximum around 90% of the cells in the liver tissue. Moreover, the scoring, which was based on the intensity and area of fluorescence-positive pixels within a single liver cell (+1 to +4), indicated a dose-dependent elevation of AAV5-GLA vDNA and GLA mRNA levels per cell.

In NHPs, liver cells also showed the presence of vDNA and GLA mRNA through FISH analysis (Figure 2B). Similarly, GLA protein was detected in the liver of NHPs after immunohistochemistry (IHC) analysis using an anti-human GLA antibody (Figure 2C). In NHPs, some background staining on FISH and IHC was detected, due to endogenous primate GLA that resembles human transgene GLA, as seen in naive tissue controls. Analysis of the spatial distribution of the FISH probe within the hepatic lobules indicated that vDNA and GLA mRNA are present throughout, with a preference for the portal vein side (Figure 2D, left panel). GLA protein was observed to be distributed more equally in the hepatic lobule, likely due to secretion from cells and to the blood flow from the portal to the central vein (Figure 2D, right panel). In GLA-KO mice, spatial
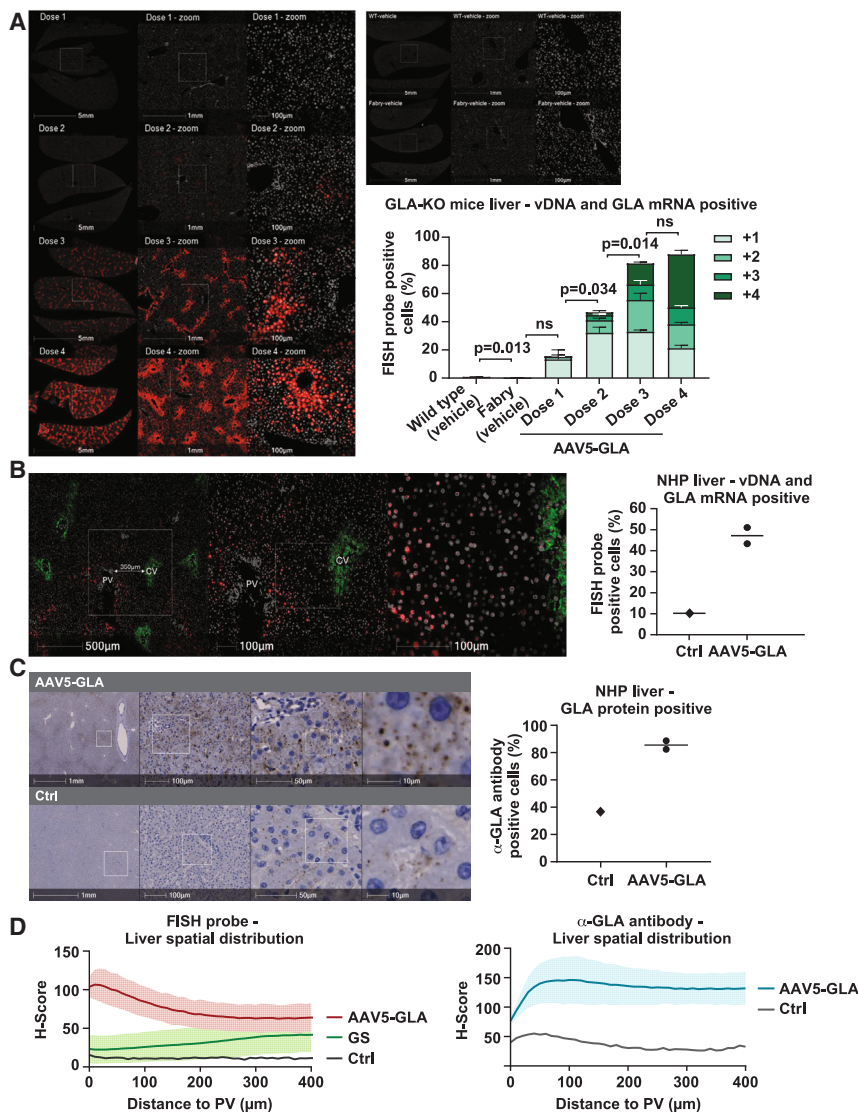
Figure 2. Robust liver transduction of AAV5-GLA in GLA-KO mice and WT NHPs

(A) Fluorescence *in situ* hybridization (FISH) analysis in livers of GLA-KO mice treated with one of four doses of AAV5-GLA (left). For comparison, WT and Fabry mice were treated with vehicle (left). The FISH probe targets both vector DNA and GLA transgene mRNA (in red). Semi-quantitative analysis of FISH staining determines the percentage and standard deviation (error bars) of FISH-probe-positive cells in liver tissue, shown on the y axis. Brown-Forsythe and Welch ANOVA with Dunnett's T3 test was used for statistical analysis on total percentage of positive cells between groups, and significance is indicated above the bars (ns, not significant). The scoring is classified into four categories: +1 if the cell contains 1–6 detected dots after segmentation based on settings for intensity, area and expected probe-size, +2 if it contains 7–20 segmented dots, +3 if there are 21–41 segmented dots per cell, and +4 if it contains 42 or more segmented dots. The scoring goes from +1 in lightest green to +4 in darkest green. The treatment groups contain 3–4 animals. (B) FISH analysis in livers of WT NHPs treated with AAV5-GLA. The FISH probe is shown in red; GS, a central vein marker, is shown in green. Semi-quantitative analysis of FISH staining determines the percentage of FISH-probe-positive cells in liver tissue. Two treated NHPs (*n* = 2) were analyzed. Naive NHP liver tissue was used as a control (Ctrl). (C) Immunohistochemical detection of GLA protein expression in the liver of NHPs, using anti-human GLA antibody. Semi-quantitative analysis of IHC staining determines the percentage anti-GLA-positive cells in liver tissue. Two treated NHPs (*n* = 2) were analyzed. Naive NHP liver tissue was used as a control (Ctrl). (D) Spatial characteristics of AAV5-GLA treatment demonstrated by FISH and IHC in the liver of NHPs. GS was used as a marker protein for the central vein. The fluorescence signal was analyzed and quantified using automated tissue detection, followed by cell segmentation, probe or antibody detection, and finally portal vein (PV) detection. This approach was used to measure the H-score at varying distances from the PV. The H-score accounts for the percentage of positive cells, including the positivity based on signal strength and area. A line indicates the average H-score, and the shaded area is the observed variation as standard error of the mean (SEM). GS, glutamine synthetase; KO, knockout; IV, intravenous; PBS, phosphate-buffered saline.

distribution analysis demonstrated the dose-responsive presence of vDNA and GLA transgene mRNA throughout the liver, with somewhat higher H-scores toward the central vein side of the functional hepatic unit (Figure S1; GLA protein not analyzed). Note that, similar to our findings, Bell et al. described an inverted zonation of AAV liver transduction between mice and NHP, the latter showing most intense expression around the portal area.[22]

AAV5-GLA biodistribution and liver-restricted transgene expression

To assess vDNA and GLA mRNA tissue distribution, DNA and mRNA isolated from organs were analyzed by RT-qPCR with primers and probes that were transgene specific or for the housekeeping gene glyceraldehyde-3-phosphate dehydrogenase (GAPDH) to assess cDNA synthesis efficacy (Figure S2). In both GLA-KO mice and NHPs, most of the vDNA and resultant mRNA were located in the liver (Figure 3), relative to the other organs analyzed (lung, adrenal gland, spleen, kidney, heart, testis, and brain in both species; also skin [fingertip, abdomen], intestine [ileum], sciatic nerve, and pancreas in NHPs). In GLA-KO mice, GLA mRNA expression was found in the lung and adrenal gland at several logs lower than in liver; in NHPs, mRNA expression was found in the adrenal gland at several logs lower than in liver. Given the liver specificity of the AAV5 capsid and the conditional expression from the novel, small and strong, liver-restricted proprietary promoter, these results were expected.[23] As a next step for Fabry disease and the mode of action of

A Mice

vDNA in tissues

GLA mRNA in tissues

B NHP

vDNA in tissues

GLA mRNA in tissues
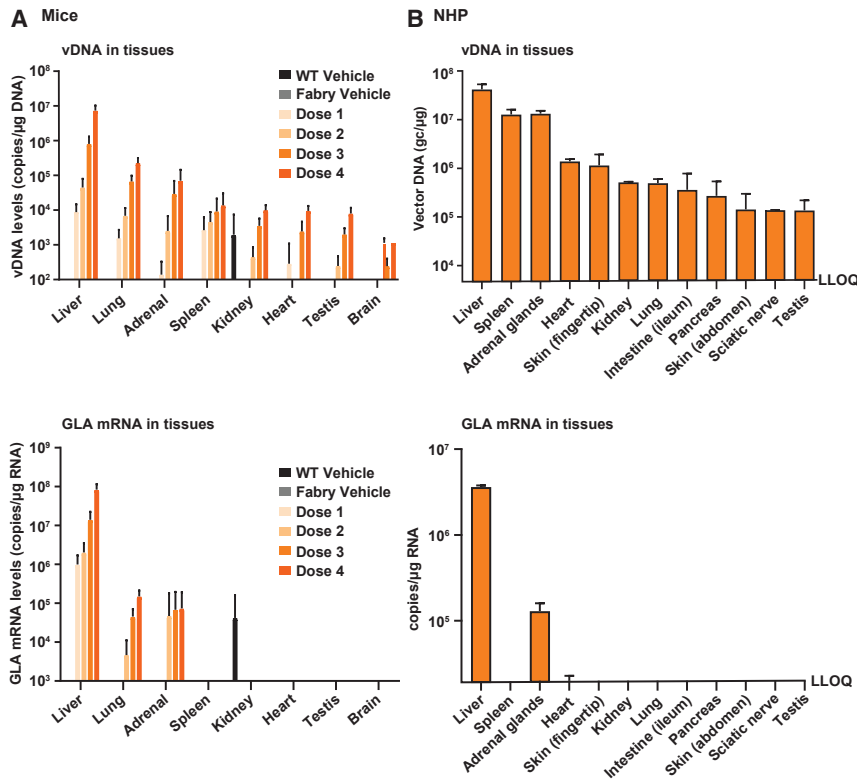
Figure 3. Biodistribution of AAV5-GLA in GLA-KO mice and NHPs

Vector DNA and GLA mRNA were isolated and measured by RT-qPCR in various organs from GLA-KO mice (A, $n = 8$) or NHP (B, $n = 2$) treated with AAV5-GLA for 12 or 8 weeks, respectively. Individual animal data points are shown as symbols, and the group average with standard deviation is shown as bars and lines. The kidney mRNA result in the WT group in mice is likely a human error and should be disregarded.

AAV5-GLA, it was important to determine whether GLA produced in the liver would be distributed to other organs to achieve function there (i.e., cross-correction). In GLA-KO mice injected with AAV5-GLA at the age of 7–8 weeks and assessed at 12 weeks post injection, not only were vDNA, GLA mRNA, and GLA enzyme activity present in a dose-dependent manner in the liver but GLA activity also was present in a dose-dependent manner in plasma (Figure 4A), indicating that the active GLA enzyme had the potential to be distributed to other organs and tissues for cross-correction. Moreover, there was a strong correlation between transgene mRNA expression and liver GLA activity that led to a strong correlation between liver and plasma GLA activity. GLA activity also was found in the liver and plasma of AAV5-GLA-treated NHPs, demonstrating stable expression and function over time (8 weeks post dosing) in a species more closely related to humans (Figure 4B).

Cross-correction analyses

GLA-KO mice treated with AAV5-GLA at 7–8 weeks of age were analyzed for GLA cross-correction in kidney and heart at 12 weeks post injection. Results demonstrated that GLA activity, as shown by measurement of active enzyme and reduction in the lyso-Gb3 and Gb3 substrates, was present in a dose-dependent manner in both kidney and heart (Figure 5). Thus, the GLA enzyme was effectively distributed via the plasma to the kidney and heart, because GLA mRNA was not previously present in those organs. At the highest doses of AAV5-GLA, substrate levels in the heart were similar to those in wild-type (WT) mice. GLA activity in the brain was minimally detectable above background levels in mice treated with the highest dose of AAV5-GLA. However, brain tissue showed significant and dose-dependent reduction of both GLA substrates, although substrate levels remained much higher than in WT mice (Figure S3 and data not shown). As expected, liver and plasma GLA substrate levels were significantly reduced in a dose-dependent manner toward WT levels (Figure S3).

When mice were analyzed at 28 weeks post injection, plasma GLA activity remained stable and substrate levels in heart and kidney remained reduced (Figure 6; results for Gb3 [not shown] were similar to lyso-Gb3), demonstrating long-term cross-correction. Further, in GLA-KO mice first treated with AAV5-GLA at a later stage of the pathological process (20 weeks of age), when the mice have a manifested nociception phenotype, measurements of plasma GLA activity and substrate levels in the heart and kidney at 16 weeks post injection also demonstrated stable plasma activity and long-term cross-correction (Figure 7; results for Gb3 [not shown] were similar to lyso-Gb3).

Improvement in nociception

Mice treated with any one of four doses of AAV5-GLA or vehicle at 7–8 weeks of age were placed onto an incremental hotplate at 10 weeks post injection to measure nociception. Average reaction time to the rising heat was 89.7 s (47.9°C) for WT mice who received vehicle and 101.8 s (49.7°C) for GLA-KO mice who received vehicle, for a difference of 12.1 s or 1.8°C. With increasing dose of AAV5-GLA, the latency to react to the rising heat stimulus normalized to WT response times, showing progressive improvement in the nociception phenotype of GLA-KO mice after treatment with AAV5-GLA (Figure 8). Nociception was also measured in mice at 26 weeks post injection (when they were over 7.5 months old) after treatment with dose 2 or dose 3 of AAV5-GLA or vehicle at 7–8 weeks of age. Average reaction time to the rising heat was 91.9 s (48.3°C) for WT mice who received vehicle and 107.1 s (50.6°C) for GLA-KO mice who received vehicle, for a difference of 15 s or 2.3°C. With increasing doses of AAV5-GLA, the latency of treated GLA-KO mice to react to the rising heat stimulus normalized toward WT response times, showing
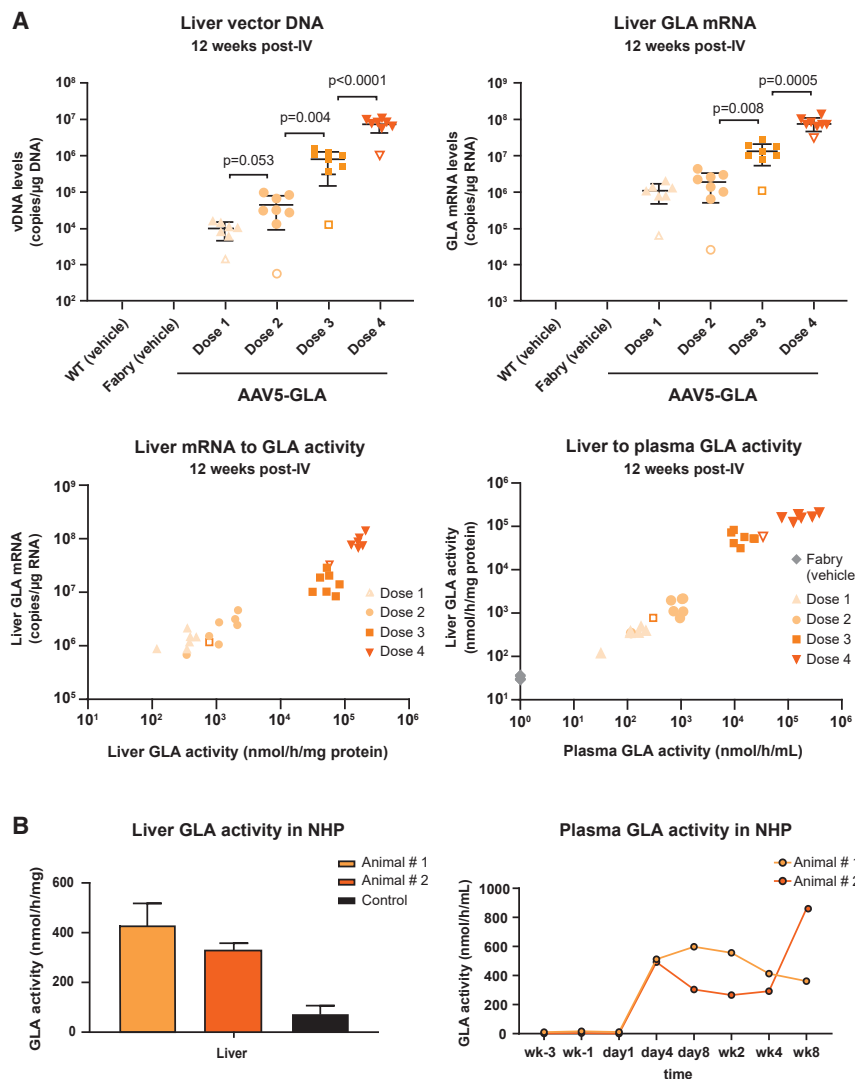
Figure 4. Production of GLA mRNA in the liver and production of active GLA enzyme in liver and plasma after AAV5-GLA treatment in GLA-KO mice and NHPs

(A) AAV5-GLA dose dependency in liver and plasma of GLA-KO mice treated with any one of four doses of AAV5-GLA ($n = 8$). Individual animal data points are shown as separate symbols; in addition, the group average with standard deviation is shown as lines. Open symbols indicate individual animals with vDNA levels more than two times the standard deviation apart from the group average. Correlations were present between GLA mRNA expression and GLA enzyme activity in the liver and between GLA enzyme activity in the liver and plasma. (B) Liver and plasma GLA activity in NHPs ($n = 2$) treated with AAV5-GLA 8 weeks post intravenous (IV) dosing. For liver, an average of the eight liver lobes with standard deviation is shown. wk, week. Open symbols indicate mice that had vDNA levels 2 standard deviations apart from the group average.

there were no notable events or adverse clinical observations in the animals, and histopathological examination (heart, kidney, liver, spleen, and testis), clinical chemistry, and hematology evaluations all indicated no adverse findings related to treatment.

DISCUSSION

AAV5-GLA is a novel gene therapy developed as a potential one-time treatment to provide long-term replacement of GLA in individuals with Fabry disease. Use of an AAV5 vector and a novel, small and strong, liver-specific promoter that localizes transgene production to the liver has the potential to provide durable enzyme production due to the slow turnover of hepatocytes.[24] A liver-specific gene therapy that uses the same validated AAV5 capsid technology as AAV5-GLA provided sustained levels of circulating transgene product in patients with hemophilia B, leading to an approved gene-therapy product (HEMGENIX [etranacogene dezaparvovec-drlb]).[1]

The AAV5 capsid has low immunogenicity, based on the low prevalence and avidity of neutralizing antibodies against it in the human population.[25,26] The pathogen-associated molecular pattern (PAMP) CpG content of the vector genome correlates strongly with long-term transgene expression, lower incidences of cytotoxic T lymphocytes (CTLs), and immunotoxicity.[27] Using the equation proposed by Wright and colleagues,[28] we quantified the PAMP CpG risk of AAV5-GLA. The normalized value for risk factor 3 (NRF_3) of the AAV5-GLA gene expression cassette and the inverted terminal repeats (ITRs), 6.35, is below the value of 6.8 described for AAV8-FIX/sc, a vector that shows durable expression in humans.[28] In

improvement in the nociception phenotype (Figure S4). In addition, when GLA-KO mice treated with AAV5-GLA at 20 weeks of age were placed onto an incremental hotplate 14 weeks post injection (the same age as the mice above), with increasing doses of AAV5-GLA, the latency of treated GLA-KO mice to react to the rising heat stimulus also shifted toward WT response times, again showing improvement in the nociception phenotype (Figure S4).

Safety

AAV5-GLA gene therapy had a favorable safety profile in both GLA-KO mice and WT NHPs. Although the GLA-KO mice studies were designed as proof-of-concept studies, histopathological examination of nine organs (testes and epididymis, spleen, liver, adrenal gland, kidney, heart, lung, brain, and skeletal muscle) showed no treatment dose-related macroscopic findings or microscopic changes. Among a total of 95 animals in the three studies, one mouse died for unknown reasons before the intravenous injection. During the NHP study,
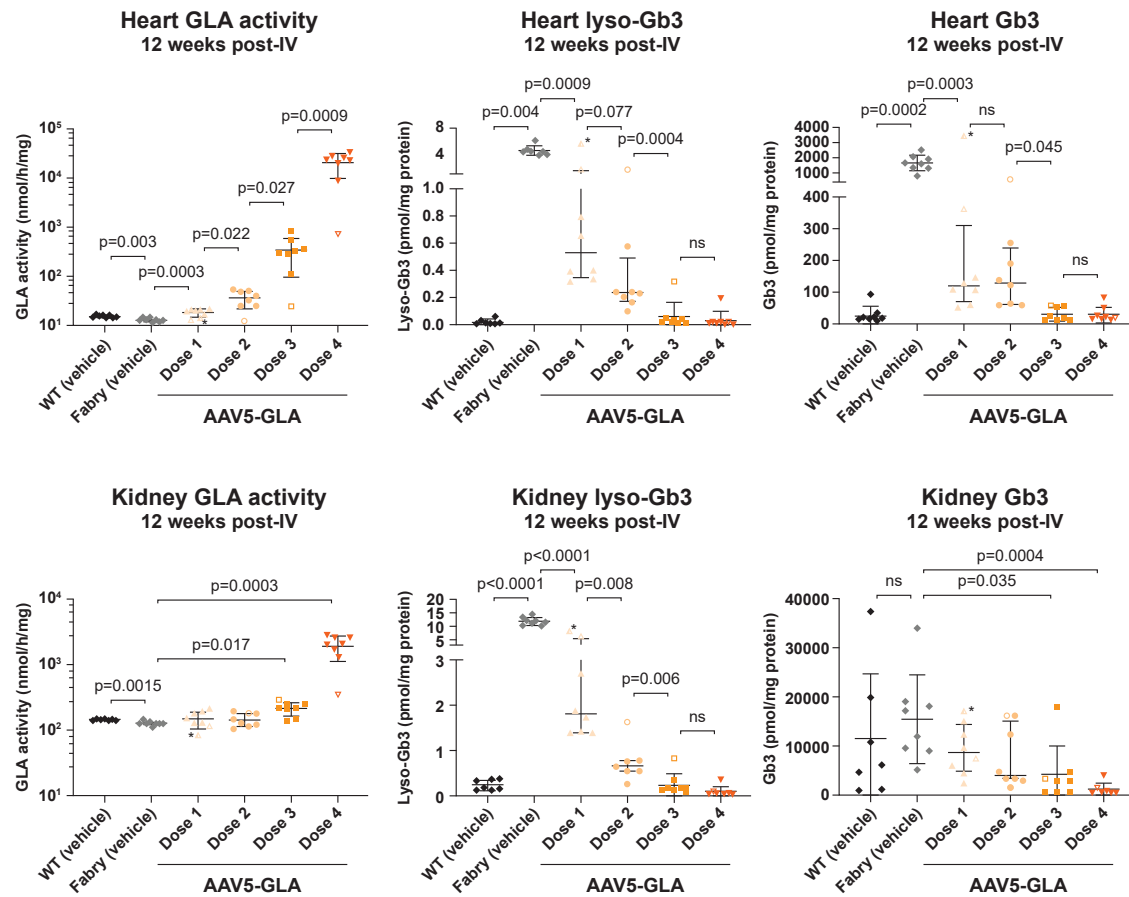
Figure 5. Dose-dependent cross-correction in kidney and heart of GLA-KO mice treated with AAV5-GLA

Kidney and heart tissue was isolated from GLA-KO mice treated with one of four doses AAV5-GLA for 12 weeks, and GLA enzyme activity and levels of the substrates Gb3 and lyso-Gb3 were determined. Individual animal data points are shown as separate symbols; in addition, the group average with standard deviation is shown as lines. Open symbols indicate individual animals with vDNA levels more than two times the standard deviation apart from the group average. Gb3, globotriaosylceramide; lyso-Gb3, globotriaosylsphingosine. Asterisks indicate one animal with vDNA and mRNA levels below the LLOQ that was removed from the dataset.

addition, the approach of liver-restricted transgene expression was chosen to limit potential immune responses to the transgene, since patients with classic Fabry disease are at risk of developing anti-drug antibodies during ERT treatment.[29,30] Others have shown sustained expression of GLA and tolerance induction using a liver-specific promoter in mice and NHPs.[15,18,31]

In GLA-KO mice, a mouse model of Fabry disease, we demonstrated that a single intravenous injection of AAV5-GLA at 7–8 weeks of age resulted in AAV5 vector transduction primarily in the liver, as demonstrated by detection of vDNA; transgene transcription, as shown by detection of GLA mRNA; and mRNA translation, as shown by detection of the GLA protein in the liver. In addition, the restriction of GLA mRNA expression mainly to the liver indicated the promoter's liver specificity. We also found that the GLA protein produced in the liver was secreted into the bloodstream, based on the presence of GLA activity in plasma, and that the enzyme could be taken up by organs such as kidney and heart,

which showed GLA activity. We confirmed cross-correction via demonstration of the reduction of GLA substrates (Gb3 and lyso-Gb3) in kidney and heart and showed that the nociception phenotype of GLA-KO mice, which reflects damage caused by accumulation of lyso-Gb3 in neurons,[31] could be improved with AAV5-GLA treatment. All of these treatment effects were sustained for more than 6 months.

Even when GLA-KO mice were not treated with AAV5-GLA until 20 weeks of age, a time point at which more substrate had accumulated and the nociception phenotype had manifested, AAV5-GLA transduced the liver, GLA mRNA was expressed, and active GLA enzyme was produced, secreted into the plasma, and taken up by the heart and kidney, where it reduced substrate levels and also improved the nociception phenotype. These findings are particularly relevant to possible treatment of patients with Fabry disease, since a diagnostic delay is often present, and patients may have significant GLA substrate accumulation and
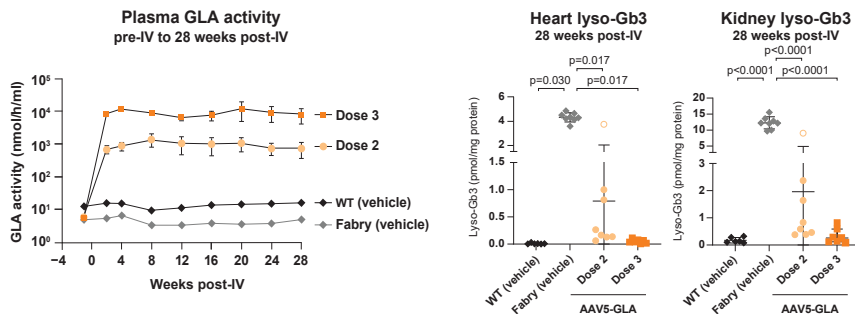
Figure 6. Sustained long-term efficacy of AAV5-GLA and cross-correction after treatment of GLA-KO mice

GLA-KO mice were treated with one of two doses of AAV5-GLA for 28 weeks (n = 7 or 8). Plasma GLA activity levels were followed over time and are shown as a group average with standard deviation. Lyso-Gb3 was assessed in kidney and heart tissues. Individual animal data points for lyso-Gb3 are shown as separate symbols; in addition, the group average with standard deviation is shown as lines. Open symbols indicate individual animals with vDNA levels more than two times the standard deviation apart from the group average.

disease manifestations by the time they begin disease-specific treatment.[32]

Findings in the NHP study supported those in the GLA-KO mice. In NHPs, a single infusion of AAV5-GLA was well tolerated, with no safety issues noted, and led to liver transduction and transgene transcription, with the highest amounts of vDNA and GLA mRNA found in the liver, confirming AAV5-GLA as a liver-specific gene therapy. Further, the strength of the novel promoter was supported by the demonstration of production of an unrelated transgene in NHPs. GLA enzyme activity in liver and plasma was sustained throughout the 8-week follow-up period. Spatial distribution analysis indicated the presence of vDNA, GLA mRNA, and GLA enzyme throughout the liver. Limitations of the NHP study include the small numbers of animals studied and the limited follow-up period; these will be investigated in future studies.

Multiple efforts are currently underway to develop gene therapy for Fabry disease, with approaches differing in the choice of AAV serotype, transgene codon optimization, and/or promoter selection. 4D Molecular Therapeutics' 4D-310 employs a cardiac-directed capsid (C102) and a ubiquitous promoter for the expression of GLA. 4D-310-treated patients in the INGLAXA phase 1/2 clinical trials have shown increased plasma GLA activity levels, and IHC on a biopsy from one patient demonstrated GLA protein presence in heart tissue.[33] However, the INGLAXA trials experienced a setback due to adverse events, as three of six patients developed atypical hemolytic uremic syndrome (aHUS). Recently, serotype AAV9 has been utilized to cross the blood-brain barrier, reaching the central

nervous system in GLA-KO mice, although confirmation in NHPs is still required.[34–36] In many cases, the GLA transgene is codon optimized, with further engineering done by Amicus and Codexis, through constructing disulfide bonds that lead to stable homodimer formation and directed evolution that has increased serum half-lives.[37,38] Two liver-directed gene therapies have reached the clinic, Sangamo's ST-920 and Freeline's FLT190, both of which use liver-restricted promoters.[39,40] FLT190 has been deprioritized, as plasma GLA activity levels in patients increased but stayed below normal levels, and two patients showed signs of mild transient myocarditis.[41] In the STAAR phase 1/2 clinical study, ST-920-treated Fabry patients exhibited increased plasma GLA activity levels and, importantly, stability in renal function.[42] Each approach has its advantages and disadvantages, which must be evaluated in clinical practice. While significant progress has been made in the development of gene therapies for Fabry disease, further clinical trials and studies are essential to determine the safest and most effective approach for patients. The ongoing research and diverse strategies underscore the complexity of treating this condition and the necessity for continued innovation and evaluation.

In conclusion, use of a novel, small, and efficient promoter driving GLA production in an AAV5-based gene therapy has shown preclinical promise for the treatment of Fabry disease. Demonstration of GLA activity in plasma, heart, and kidney of GLA-KO mice established that GLA produced in the liver was effectively secreted into the bloodstream and was taken up by target organs to remove accumulated substrates and improve nociception. In NHPs, GLA activity in the liver and plasma and tolerability over 8 weeks further support
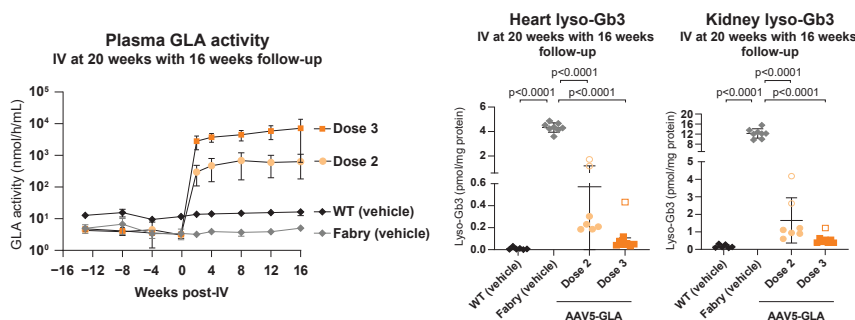
Figure 7. Sustained efficacy of AAV5-GLA and cross-correction after later-in-life treatment of GLA-KO mice

GLA-KO mice were treated at 20 weeks of age with one of two doses AAV5-GLA for 16 weeks (n = 7 or 8). Plasma GLA activity levels were followed over time and are shown as a group average with standard deviation. Lyso-Gb3 was assessed in kidney and heart tissues. Individual animal data points for lyso-Gb3 are shown as separate symbols; in addition, the group average with standard deviation is shown as lines. Open symbols indicate individual animals with vDNA levels more than two times the standard deviation apart from the group average.

Nociception
10 weeks post-IV
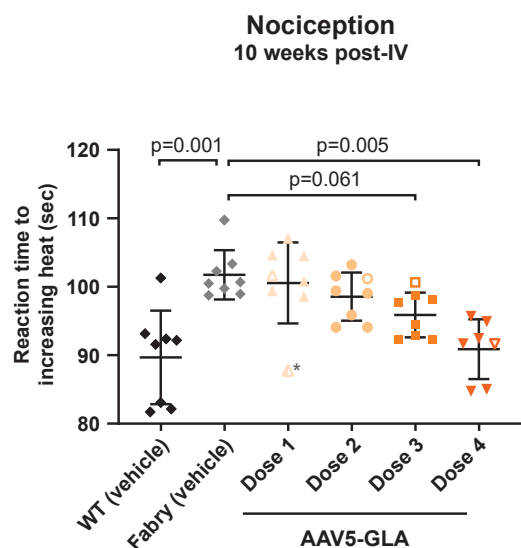
Figure 8. Nociception phenotype improvement, assessed using an incremental hotplate assay, with increasing doses of AAV5-GLA in GLA-KO mice

GLA-KO mice were treated with any one of four doses of AAV5-GLA for 12 weeks (n = 8). Individual animal data points on the reaction time to increasing heat are shown as separate symbols; in addition, the group average with standard deviation is shown as lines. Open symbols indicate individual animals with vDNA levels more than two times the standard deviation apart from the group average. The asterisk indicates one animal with vDNA and mRNA levels below the LLOQ that was removed from the dataset.

the investigation of AAV5-GLA in future studies. The data support the development of such an approach in Fabry disease, and AAV5-GLA (as AMT-191) clinical studies with a phase 1/2, open-label, multicenter trial design have been initiated to evaluate safety and biomarkers of efficacy in adult males with Fabry disease (NCT06270316).

MATERIALS AND METHODS
Vector design and production

AAV5-GLA is an AAV5 capsid-based vector containing the cDNA of the WT human GLA enzyme that is defective in Fabry disease. In the mouse studies, transgene expression was under the control of the liver-restricted proprietary promoter C7′ (AMT-191). The vector has an SV40-poly(A) signal sequence for mRNA stability, and the expression cassette is flanked by ITRs for encapsidation into the AAV5 capsid and concatemer formation (Figure 1). In the NHP studies, an earlier version of the C7′ promoter (C7) was used. C7 is a slightly shorter version of C7′.

Analysis of transgene protein production for liver promoter comparison

Cynomolgus monkeys (n = 2 per group) received intravenous administration of 9×10^{13} gc/kg of an AAV5-containing unrelated transgene under the control of the LP1 or C7 promoter. Transduction of the vector containing the $\sim$550-base-pair LP1 promoter, which comprises core liver-specific elements of the human apolipoprotein hepat-

ic control region (HCR), the human alpha-1 antitrypsin (hAAT) gene promoter, and an SV40 intron,[19] served as a reference. Plasma samples were obtained at various times from 2 weeks prior to dosing to 16 weeks post injection for measurement of transgene protein secretion into plasma. Measurement was carried out with a transgene-specific sandwich enzyme-linked immunosorbent assay (ELISA). Plasma samples were diluted 100-fold or more and loaded for capture onto an ELISA plate coated with antigen-specific monoclonal antibody. Detection was performed using a peroxidase-labeled anti-human antibody followed by colorimetric reaction. All samples were measured in duplicate.

Mice

The original GLA-KO mouse model,[20] which has a hybrid background (129/SvJ x C57BL/6), contains a knockout for murine GLA. For the current studies, GLA-KO mice were obtained on a C57BL/6 background, for a consistent genetic origin; WT littermates were used as controls. Animals were provided by collaborators at Medical Biochemistry, Amsterdam UMC, University of Amsterdam.

Each treatment group contained a total of eight animals, except for the WT vehicle group used in the long-term study and in the later-in-life treatment study, as only seven WT animals were available in the breeding colony at the time. All animals except for those in the vehicle groups received an intravenous injection of AAV5-GLA into the tail vein at 7–8 weeks of age for systemic distribution of the vector. Animals were injected with 190 μL of dose 1, 2, and 3 and 200 μL of dose 4. Final concentrations of doses 1, 2, 3, and 4 were 9.84×10^{11} gc/mL, 4.92×10^{12} gc/mL, 2.44×10^{13} gc/mL, and 7.7×10^{14} gc/mL, respectively. Previous studies have shown that injection of GLA-KO mice with AAV-GLA vectors at 4, 12, and 16 weeks reduced Gb3 in liver, kidney, heart, and spleen at 3 months post administration,[31,43,44] providing the rationale for follow-up periods of 12 and 28 weeks in the current studies. In addition, because hemizygous male GLA-KO mice have a latent thermal nociceptive response phenotype that may be related to the neuropathic pain and impaired temperature perception experienced by individuals with Fabry disease,[45,46] we performed our studies in male mice.

For the later-in-life analyses, GLA-KO mice were injected with AAV5-GLA at 20 weeks of age, since accumulation of Gb3 does not increase extensively after that age.[47] In contrast, plasma levels of lyso-Gb3 continue to increase at 10, 20, and 35 weeks of age.[21] The nociception phenotype becomes apparent around 5 months of age.[31,48,49] In our previous experience, GLA-KO mice developed heat hyposensitivity at 18 weeks of age and showed high levels of Gb3 and lyso-Gb3 accumulation at 20 weeks of age in several organs (data not shown); thus, to assess an effect of AAV5-GLA when the nociception phenotype becomes apparent, we chose the age of 20 weeks for treatment. Animals were followed for 16 weeks (including the nociception test at 14 weeks), to the same age as those in the long-term expression study (36 weeks), for prospective comparison purposes.

All procedures adhered to international or Dutch standards for the care and use of laboratory animals. Approval for the murine studies was given by an animal welfare and ethics committee prior to the start of the work in the animal facility of Amsterdam UMC, the Netherlands.

Cynomolgus macaques

Experimentally naive, specific pathogen-free (SPF), male cynomolgus macaques (*Macaca fascicularis*) weighing 2.45–3.10 kg were studied. Animals received a 30-min infusion of AAV5-GLA at a dose of 9×10^{13} gc/kg through a cannula inserted into the saphenous vein. The health of the NHP was closely monitored for the duration of the study with a standardized score sheet encompassing items such as general body condition, motor activity, and central nervous system observations.

The study was approved by the Niedersächsisches Landesamt für Verbraucherschutz und Lebensmittelsicherheit (LAVES; Oldenburg, Germany) and the institutional Tierschutzausschuss (IACUC), prior to the initiation of the in-life phase.

Analytical procedures

Plasma and tissue sample collection

Blood was collected in EDTA-coated tubes and placed on ice. After centrifugation at $2{,}500 \times g$ for 20 min at 4°C (mice) or $1{,}500 \times g$ for 10 min (NHP), plasma was collected and stored at −80°C until analysis. For IHC and pathology observation, organs were fixed in 4% paraformaldehyde. For pathology assessment of mouse tissues, paraffin-embedded tissue blocks were shipped to AnaPath Services, Switzerland, where they were cut at a thickness of ∼2–4 μm, stained with hematoxylin and eosin, and examined under a light microscope by the study pathologist. Paraformaldehyde-fixed NHP tissues were shipped to Morphisto for processing to wax blocks, which were shipped to Charles River (Edinburgh), processed to hematoxylin and eosin-stained slides, and underwent microscopic evaluation by a board-certified veterinary pathologist.

Most mouse organs were snap frozen for bioanalysis. Snap-frozen mouse tissues were crushed with the CryoPREP system type CP02 (Covaris). Pulverized tissues were lysed in Lysing Matrix D tubes (MP Biomedicals) with ethanol and β-mercaptoethanol (Sigma) using the TissueLyser II (QIAGEN). DNA and RNA were extracted using the AllPrep DNA/RNA 96 kit (QIAGEN) according to the manufacturer's protocol. DNA and RNA were quantified with the NanoPhotometer N120 (IMPLEN) by measuring nucleic acid concentrations and purity ratios in duplicate. Samples were stored at −80°C until analysis. For Gb3 and lyso-Gb3 determination, pulverized tissues were lysed in water by sonication on ice (40% amplitude for three cycles of 10 s on and 20 s off) with a Vibra-Cell VCX 130 (Sonics, Newtown, CT, USA). Total protein concentration was determined using a Pierce BCA protein assay kit (Thermo Fisher Scientific, Waltham, MA, USA) and measured using an EMax Plus microplate reader (Molecular Devices, Sunnyvale, CA, USA).

FISH

Detection of vDNA and human GLA transgene mRNA in mice was performed with the manual ACD RNAScope Multiplex v2 Kit (ACD, UK, catalog #323110) following the manufacturer's protocol for FFPE-tissue with minor adjustments for protease treatment and diluting secondary Cy3 1:1500 in TSA buffer. Nuclei were counterstained with the in-kit DAPI solution, and slides were mounted with ProLong Gold antifade (Thermo Fisher Scientific, Waltham, MA, USA, P36934). Liver images were acquired with the AxioScan Z1 Slide scanner (Zeiss, Germany) with a 40×/0.95NA Plan-Apochromat objective and analyzed within HALO software (IndicaLabs, Albuquerque, NM, USA; v3.4). Image analysis included a series of AI-based classifiers for tissue detection, nuclei segmentation, and portal vein annotation followed by quantification of the overall percentage of vDNA and GLA mRNA-positive cells and calculation of the H-score using FISH-Plugin v3.1.3 of the HALO software. Spatial analysis was performed with the infiltration assay plugin to quantify probe-positive cells in dependency on the distance of the portal veins. For data representation, GraphPad Prism v9.3.1 was used. For spatial analysis, the mean H-score was plotted as an x-y graph with standard errors of the mean for variation.

In NHPs, sections of liver were analyzed for vDNA and GLA mRNA. Sections (4 μm) were cut with a microtome (Leica RM2255) and mounted onto slides for FISH with a probe specific for vDNA and GLA mRNA, using a kit from ACDbio, to determine the expression pattern. For quantification of the vDNA and GLA mRNA within the samples stained via FISH in the Cy5 channel, HALO v3.1.1076.325 software was used. First, an AI DenseNet classifier was used to define the tissue analyzed, with the exclusion of folds or out-of-focus areas. A resolution of 1.85 μm/pixel and a minimum object size of 120 μm^2 was set, and every area above a probability threshold of 80 was added to the tissue annotation layer. Within the annotation layer, the FISH v2.1.10 plugin was used for single-cell-based quantification. For cell detection, the DAPI channel was used with a nuclear contrast threshold of 0.496, a minimum nuclear intensity of 0.09, and a segmentation aggressiveness of 0.65. For the spatial distribution of the scored cells, an AI DenseNet classifier was used to add an annotation layer around the portal veins within the tissue annotation layer. The detected cells from the FISH plugin were used in the infiltration assay to calculate the amount of negative, positive, scored, and glutamine synthetase (GS)-positive cells as cells/objects inside of the AI-defined tissue annotations, with the AI-classified portal vein annotations as the interface layer.

Immunohistochemical detection of GLA protein expression in NHP liver

Sections of NHP liver were analyzed for expression of the GLA protein by IHC. After deparaffinization in xylene and graded ethanol solutions (100%, 96%, and 70% ethanol), sections were washed twice in distilled water, incubated in antigen retrieval buffer (Tris-EDTA, pH 9) at 95°C for 30 min, and cooled for 30 min at room temperature. After three 1-min washes in distilled water, sections were incubated for 20 min with 3% hydrogen peroxide in phosphate-buffered saline

(PBS) to block endogenous peroxidase, washed three times (3-min washes) with 0.1% Tween/PBS, and incubated with 5% bovine serum albumin (BSA)/5% normal goat serum (NGS) in PBS for 30 min. Sections were then incubated overnight at 4°C with an anti-GLA antibody (Thermo Fisher Scientific, Waltham, MA, USA, MA5-29309) at a 1:4,000 dilution in PBS/1% BSA/1% NGS. After three 3-min washes in 0.1% Tween/PBS, sections were incubated for 30 min in Envision, washed three times (3-min washes) in 0.1% Tween/PBS, rinsed in distilled water, and developed with 3,3′-diaminobenzidine/peroxidase for up to 10 min. After the reaction was stopped with distilled water, sections were counterstained with hematoxylin and dehydrated in graded ethanol solutions (70%, 96%, and 100%) followed by xylene and mounted with rapid-mounting medium (Entellan, Merck).

qPCR for vDNA quantification

Mouse DNA samples were diluted to a set concentration (depending on extraction yield) to ensure the same input for the qPCR. A TaqMan assay with specific primers and probe for the SV40 poly(A) region (Eurofins) present in the AAV5-GLA vector was used for absolute quantification with TaqMan Universal PCR Master Mix, no AmpErase UNG (Applied Biosystems). A standard curve was prepared from 10 dilutions of linearized plasmid containing the AAV5-GLA vector genome encoding the *GLA* gene. qPCR was performed using a QuantStudio 5 Real-Time PCR System (Thermo Fisher Scientific, Waltham, MA, USA). The LLOQ was defined as 50 gc per reaction with 250 ng of DNA input (200 copies/μg DNA) during assay qualifications. During sample analysis, the LLOQ ranged between 250 and 2,400 copies/μg DNA, depending on the amount of DNA input per reaction.

For NHP DNA samples, 200 ng of isolated genomic DNA was subjected to qPCR using primers and TaqMan probe designed to amplify a sequence on the vector genome specific for SV40 poly(A). For liver samples, the copy numbers were too high (above the plasmid standard line [PSL]), so another qPCR was performed with 20 ng of DNA. As the quantification standard, a linearized DNA PSL was used. For quantification, serial dilutions of this linearized plasmid containing the qPCR target sequence were subjected to qPCR in parallel. From the results of the PSL, a calibration curve was established by linear regression. The amount of vDNA in the samples was calculated by interpolation from the calibration curve and reported as gc/μg of genomic DNA. The range of the PSL was 1×10^2 to 1×10^8 copies per reaction. The assay has an LLOQ of 1×10^2 transgene copies/20 ng DNA, which corresponds to 5×10^3 copies per μg of DNA.

RT-qPCR for mRNA quantification

Mouse RNA samples were diluted to a set concentration (depending on extraction yield) to ensure the same input for a two-step RT-qPCR. dsDNase treatment and RT were performed with Maxima First Strand cDNA Synthesis Kit for RT-qPCR, with dsDNase (Thermo Scientific) following the manufacturer's protocol and using a Biometra TAdvanced thermocycler (Westburg). cDNA was diluted 1:8,

and TaqMan Universal PCR Master Mix, no AmpErase UNG (Applied Biosystems) was used with primers and a probe targeting the GLA transgene mRNA or GAPDH mRNA. For GLA, the sequences of forward and reverse primers were 5′-CTTCCCTGGGAG TTTTGGATACTAC-3′ and 5′-CATGTGCTTATAACCATCTGC CAAA-3′, and the sequence of the probe was 5′-CAGACCTTTGCT GACTGGGGAGTAGATCTGCTA-3′. A TaqMan FAM Dye/MGB probe and the FAM Dye/MGB probe to GAPDH were used. The NHP assay ID was Rh02621745-g1, and the murine assay ID was mm9999915_g1 (Thermo Fisher Scientific, Waltham, MA, USA). For absolute quantification, 10 dilutions of the linearized plasmid were prepared. qPCR was performed using a QuantStudio 5 Real-Time PCR System (Thermo Fisher Scientific, Waltham, MA, USA). The LLOQ was defined as 12.5 molecules per reaction with 10 ng RNA input (1,250 copies/μg RNA). During sample analysis, the LLOQ ranged between 2,450 and 892,857 copies/μg RNA, depending on the amount of RNA input per reaction.

NHP RNA was added to a cDNA synthesis reaction using Maxima First Strand cDNA synthesis kit (K1672, Thermo Fisher Scientific, Waltham, MA, USA). Subsequently, 20–200 ng cDNA was subjected to qPCR using primers designed to amplify a sequence unique to the GLA cDNA. The input of RNA per qPCR reaction was 8 ng for all samples, except for sciatic nerve samples due to very low RNA yields from this tissue. However, all final values were reported as gc/μg of total RNA. As the quantification standard, a PSL plasmid was used. For quantification, serial dilutions of this linearized plasmid containing the qPCR target sequence were subjected to qPCR in parallel to the samples. From the results of the plasmid dilutions, a calibration curve was established by linear regression. Specific RNA copies in the samples were calculated by interpolation from the calibration curve and reported as gc per μg of RNA. The range of the PSL was 2×10^2 to 2×10^8 copies (ssDNA) per reaction. The assay has an LLOQ of 2×10^4 transgene copies/μg RNA.

GLA enzyme activity

In mouse and NHP plasma and tissue lysates, GLA activity was determined with an assay that measures the enzyme's cleavage activity utilizing the synthetic fluorogenic 4-methylumbelliferyl-α-D-galactopyranoside (4-MU-α-GLA) substrate, which, upon cleavage, liberates 4-MU, which was measured with a fluorescence plate reader. Samples or standards (10 μL) were incubated with 20 μL of assay buffer containing 4 MU-αGLA substrate and galNac (5 mM 4-MU-α-gal, 0.1 M galNac in 50 mM sodium citrate, 50 mM NaCl, pH 4.0) at 37°C. The reaction was stopped by adding 200 μL of stop solution (0.2 M glycine-NaOH, pH 10.7). The fluorescence of 4-MU after hydrolysis was measured at an excitation wavelength of 355 nm and emission wavelength of 460 nm. The molar quantities of produced 4-MU by GLA in the samples were calculated by linear regression of a 4-MU standard line.

Gb3 and Lyso-Gb3 determination

Gb3 and lyso-Gb3 were measured as previously described,[50] with a modification of the Bligh and Dyer method. Briefly, 100 pmol of

C17-dh-ceramide and 2 pmol of $^{13}C_5$-lyso-Gb3 (Bio-Organic Synthesis Department, University Leiden, the Netherlands) were added to tissue samples (25 μL of kidney or heart homogenate, 10 μL of plasma), and lipids were extracted with methanol, chloroform, and ammonium formate buffer (1:1:0.9; v/v/v). The resulting upper phase (lyso-Gb3) was dried under a N_2 stream and further extracted with water/butanol (1:1; v/v) before being subjected to ultra-high-performance liquid chromatography-mass spectrometry (UPLC-MS). Gb3, in the lower phase, was further deacylated with methanolic NaOH (0.1 M) in a microwave SAM-155, CEM Corporation (Matthews, NC, USA). Deacylated lipids were further extracted with water/butanol (1:1; v/v) before being applied to the UPLC-MS.

Lipids were separated by reverse-phase liquid chromatography in liquid chromatography-tandem mass spectrometry (LC-MS/MS) with a BEH C18 column, 2.1 × 50 mm with 1.7-μm particle size (Waters) at 23°C. Mass spectrometry detection was performed in a positive mode using an electrospray ionization (ESI) source with a Xevo TQS micro instrument (Waters Corporation, Milford, MA, USA). Data were analyzed with MassLynx 4.2 software (Waters Corporation, Milford, MA, USA).

Nociception phenotype evaluation in GLA-KO mice

To assess phenotypic improvement of Fabry symptoms, all mice were subjected to a hot/cold plate test that measures the sensitivity of the nerve endings in the paws. Animals were placed on an incremental hotplate, the temperature of which rises 9°C per minute, and the average time to reaction (first jumping or licking or shaking/vibrating of the hind legs) was measured.

Statistical analysis

Mouse studies

Data from animals with a vDNA Z score above 2 (vDNA levels that are 2 standard deviations apart from the group average) were excluded from the statistical analyses. One animal with vDNA and mRNA levels below the LLOQ was removed from the dataset. Statistical analyses were performed with GraphPad Prism 9.3.1 software (Boston, MA, USA) and the following step-by-step plan: First, the dataset was tested for normality of each treatment group using the Shapiro-Wilk test. If all were Gaussian distributed, then Bartlett's test for equal variances was performed. When standard deviations were not significantly different, an unpaired t test or an ordinary one-way analysis of variance (ANOVA) was used to determine statistical differences between treatment groups corrected with Sidak's test for multiple comparisons. If standard deviations were significantly different, Welch's t test or Brown-Forsythe and Welsch ANOVA with Dunnett's T3 test for multiple comparisons was used to test for significance.

When more than one treatment group within a dataset was not Gaussian distributed, data transformation was considered. Box-Cox was performed per treatment group within the dataset, then lambda was compared within an analysis readout and between the three animal experiments for consistency. For most analysis readouts, a lambda of 0 was chosen, only for lyso-Gb3 levels, a lambda of −0.5

was selected as a better fit, following lambda data would be log Y or $1/\sqrt{Y}$ transformed, respectively. After data transformation, the dataset was tested for Gaussian distribution again in the Shapiro-Wilk test, etc. If after transformation, the data were still not forced into a normal distribution, statistical analysis was performed with a nonparametric test, ranking the data points. The Kruskal-Wallis test with Dunn's multiple comparison correction was applied to the nociception dataset in the dose-response study.

NHP study

Linear regression analyses were performed with GraphPad Prism 9 software (Boston, MA, USA). An unpaired parametric two-tailed t test with Welch's correction was used to determine statistical significance.

DATA AND CODE AVAILABILITY

ACKNOWLEDGMENTS

AUTHOR CONTRIBUTIONS

Study design, J.M.P.L. and Y.P.L.; principal investigator, J.M.P.L.; study investigator, J.M.P.L., E.A.S., Y.P.L., and R.O.; collection and assembly of data, E.A.S., G.B., L.K.S., L.P., N.E., R.O., and M.J.F.; data analysis, J.M.P.L.; data interpretation, all authors; manuscript preparation, J.M.P.L. and M.M.E.; manuscript review and revisions, all authors; final approval of manuscript, all authors.

DECLARATION OF INTERESTS

SUPPLEMENTAL INFORMATION

REFERENCES

1. Von Drygalski, A., Giermasz, A., Castaman, G., Key, N.S., Lattimore, S., Leebeek, F.W.G., Miesbach, W., Recht, M., Long, A., Gut, R., et al. (2019). Etranacogene dezaparvovec (AMT-061 phase 2b): normal/near normal FIX activity and bleed cessation in hemophilia B. Blood Adv. *3*, 3241–3247.

2. He, X., Urip, B.A., Zhang, Z., Ngan, C.C., and Feng, B. (2021). Evolving AAV-delivered therapeutics towards ultimate cures. J. Mol. Med. *99*, 593–617.

3. Issa, S.S., Shaimardanova, A.A., Solovyeva, V.V., and Rizvanov, A.A. (2023). Various AAV serotypes and their applications in gene therapy: an overview. Cells *12*, 785.

4. Germain, D.P. (2010). Fabry disease. Orphanet J. Rare Dis. *5*, 30.

5. Vardarli, I., Rischpler, C., Herrmann, K., and Weidemann, F. (2020). Diagnosis and screening of patients with Fabry disease. Therapeut. Clin. Risk Manag. *16*, 551–558.

6. Amodio, F., Caiazza, M., Monda, E., Rubino, M., Capodicasa, L., Chiosi, F., Simonelli, V., Dongiglio, F., Fimiani, F., Pepe, N., et al. (2022). An overview of molecular mechanisms in Fabry disease. Biomolecules *12*, 1460.

7. Torra, R. (2008). Renal manifestations in Fabry disease and therapeutic options. Kidney Int. Suppl. S29–S32.

8. Waldek, S., Patel, M.R., Banikazemi, M., Lemay, R., and Lee, P. (2009). Life expectancy and cause of death in males and females with Fabry disease: findings from the Fabry Registry. Genet. Med. *11*, 790–796.

9. Bernardes, T.P., Foresto, R.D., and Kirsztajn, G.M. (2020). Fabry disease: genetics, pathology, and treatment. Rev. Assoc. Med Bras (1992) *66*, s10–s16.

10. Germain, D.P., Altarescu, G., Barriales-Villa, R., Mignani, R., Pawlaczyk, K., Pieruzzi, F., Terryn, W., Vujkovac, B., and Ortiz, A. (2022). An expert consensus on practical clinical recommendations and guidance for patients with classic Fabry disease. Mol. Genet. Metabol. *137*, 49–61.

11. (2023). Fabrazyme [package Insert] (Genzyme Corporation).

12. Miesbach, W., Meijer, K., Coppens, M., Kampmann, P., Klamroth, R., Schutgens, R., Tangelder, M., Castaman, G., Schwäble, J., Bonig, H., et al. (2018). Gene therapy with adeno-associated virus vector 5-human factor IX in adults with hemophilia B. Blood *131*, 1022–1031.

13. Pipe, S.W., Leebeek, F.W.G., Recht, M., Key, N.S., Castaman, G., Miesbach, W., Lattimore, S., Peerlinck, K., Van der Valk, P., Coppens, M., et al. (2023). Gene therapy with etranacogene dezaparvovec for hemophilia B. N. Engl. J. Med. *388*, 706–718.

14. Franco, L.M., Sun, B., Yang, X., Bird, A., Zhang, H., Schneider, A., Brown, T., Young, S.P., Clay, T.M., Amalfitano, A., et al. (2005). Evasion of immune responses to introduced human acid alpha-glucosidase by liver-restricted expression in glycogen storage disease type II. Mol. Ther. *12*, 876–884.

15. Ziegler, R.J., Lonning, S.M., Armentano, D., Li, C., Souza, D.W., Cherry, M., Ford, C., Barbon, C.M., Desnick, R.J., Gao, G., et al. (2004). AAV2 vector harboring a liver-restricted promoter facilitates sustained expression of therapeutic levels of alpha-galactosidase A and the induction of immune tolerance in Fabry mice. Mol. Ther. *9*, 231–240.

16. Ishiwata, A., Mimuro, J., Mizukami, H., Kashiwakura, Y., Takano, K., Ohmori, T., Madoiwa, S., Ozawa, K., and Sakata, Y. (2009). Liver-restricted expression of the canine factor VIII gene facilitates prevention of inhibitor formation in factor VIII-deficient mice. J. Gene Med. *11*, 1020–1029.

17. Cooper, M., Nayak, S., Hoffman, B.E., Terhorst, C., Cao, O., and Herzog, R.W. (2009). Improved induction of immune tolerance to factor IX by hepatic AAV-8 gene transfer. Hum. Gene Ther. *20*, 767–776.

18. Nietupski, J.B., Hurlbut, G.D., Ziegler, R.J., Chu, Q., Hodges, B.L., Ashe, K.M., Bree, M., Cheng, S.H., Gregory, R.J., Marshall, J., and Scheule, R.K. (2011). Systemic administration of AAV8-α-galactosidase A induces humoral tolerance in nonhuman primates despite low hepatic expression. Mol. Ther. *19*, 1999–2011.

19. Nathwani, A.C., Gray, J.T., Ng, C.Y.C., Zhou, J., Spence, Y., Waddington, S.N., Tuddenham, E.G.D., Kemball-Cook, G., McIntosh, J., Boon-Spijker, M., et al. (2006). Self-complementary adeno-associated virus vectors containing a novel liver-specific human factor IX expression cassette enable highly efficient transduction of murine and nonhuman primate liver. Blood *107*, 2653–2661.

20. Ohshima, T., Murray, G.J., Swaim, W.D., Longenecker, G., Quirk, J.M., Cardarelli, C.O., Sugimoto, Y., Pastan, I., Gottesman, M.M., Brady, R.O., and Kulkarni, A.B.

21. (1997). Alpha-Galactosidase A deficient mice: a model of Fabry disease. Proc. Natl. Acad. Sci. USA *94*, 2540–2544.

21. Aerts, J.M., Groener, J.E., Kuiper, S., Donker-Koopman, W.E., Strijland, A., Ottenhoff, R., van Roomen, C., Mirzaian, M., Wijburg, F.A., Linthorst, G.E., et al. (2008). Elevated globotriaosylsphingosine is a hallmark of Fabry disease. Proc. Natl. Acad. Sci. USA *105*, 2812–2817.

22. Bell, P., Wang, L., Gao, G., Haskins, M.E., Tarantal, A.F., McCarter, R.J., Zhu, Y., Yu, H., and Wilson, J.M. (2011). Inverse zonation of hepatocyte transduction with AAV vectors between mice and non-human primates. Mol. Genet. Metabol. *104*, 395–403.

23. Majowicz, A., Salas, D., Zabaleta, N., Rodríguez-Garcia, E., González-Aseguinolaza, G., Petry, H., and Ferreira, V. (2017). Successful repeated hepatic gene delivery in mice and non-human primates achieved by sequential administration of AAV5(ch) and AAV1. Mol. Ther. *25*, 1831–1842.

24. Kattenhorn, L.M., Tipper, C.H., Stoica, L., Geraghty, D.S., Wright, T.L., Clark, K.R., and Wadsworth, S.C. (2016). Adeno-associated virus gene therapy for liver disease. Hum. Gene Ther. *27*, 947–961.

25. Majowicz, A., van Waes, F., Timmer, N., van Deventer, S.J., and Ferreira, V. (2020). Prevalence and affinity/avidity assessment of pre-existing NABs against AAV1, 2, 5 and 8 analyzed in the serum of 300 healthy donors. Haemophilia *26*, 53. [abstract P054].

26. Majowicz, A., Van Waes, F., Timmer, N., Van Deventer, S.J., and Ferreira, V. (2020). Prevalence and affinity/avidity assessment of pre-existing neutralizing antibodies (NABs) against adeno-associated virus (AAV) vector serotypes 2, 5 and 8 analyzed in the serum of 300 healthy donors. Res Pract Thromb Haemost *4*, 557–558. [abstract PB1101].

27. Wright, J.F. (2020). Codon modification and PAMPs in clinical AAV vectors: the tortoise or the hare? Mol. Ther. *28*, 701–703.

28. Wright, J.F. (2020). Quantification of CpG motifs in rAAV genomes: avoiding the toll. Mol. Ther. *28*, 1756–1758.

29. Linthorst, G.E., Hollak, C.E.M., Donker-Koopman, W.E., Strijland, A., and Aerts, J.M.F.G. (2004). Enzyme therapy for Fabry disease: neutralizing antibodies toward agalsidase alpha and beta. Kidney Int. *66*, 1589–1595.

30. Lenders, M., Neußer, L.P., Rudnicki, M., Nordbeck, P., Canaan-Kühl, S., Nowak, A., Cybulla, M., Schmitz, B., Lukas, J., Wanner, C., et al. (2018). Dose-dependent effect of enzyme replacement therapy on neutralizing antidrug antibody titers and clinical outcome in patients with Fabry disease. J. Am. Soc. Nephrol. *29*, 2879–2889.

31. Ziegler, R.J., Cherry, M., Barbon, C.M., Li, C., Bercury, S.D., Armentano, D., Desnick, R.J., and Cheng, S.H. (2007). Correction of the biochemical and functional deficits in Fabry mice following AAV8-mediated hepatic expression of α-galactosidase A. Mol. Ther. *15*, 492–500.

32. Schiffmann, R., Warnock, D.G., Banikazemi, M., Bultas, J., Linthorst, G.E., Packman, S., Sorensen, S.A., Wilcox, W.R., and Desnick, R.J. (2009). Fabry disease: progression of nephropathy, and prevalence of cardiac and cerebrovascular events before enzyme replacement therapy. Nephrol. Dial. Transplant. *24*, 2102–2111.

33. Thomas, M. (2024). Phase 1/2 clinical trial evaluating 4D-310 in adults with Fabry disease cardiomyopathy: interim analysis of cardiac and safety outcomes in patients with 12-33 months of follow-up [oral presentation]. Presented at. Annual WORLDSymposium.

34. Hayashi, Y., Sehara, Y., Watano, R., Ohba, K., Takayanagi, Y., Muramatsu, K., Sakiyama, Y., and Mizukami, H. (2023). Therapeutic strategy for Fabry disease by intravenous administration of adeno-associated virus 2 or 9 in α-galactosidase A-deficient mice. J. Gene Med. *25*, e3560.

35. Biferi, M.G., Cohen-Tannoudji, M., García-Silva, A., Souto-Rodríguez, O., Viéitez-González, I., San-Millán-Tejado, B., Fernández-Carrera, A., Pérez-Márquez, T., Teijeira-Bautista, S., Barrera, S., et al. (2021). Systemic treatment of Fabry disease using a novel AAV9 vector expressing α-Galactosidase A. Mol. Ther. Methods Clin. Dev. *20*, 1–17.

36. Boukharov, N., Yuan, S., Ruangsirluk, W., Ayyadurai, S., Rahman, A., Rivera-Hernandez, M., Sunkara, S., Tonini, K., Park, E.Y.H., Deshpande, M., and Islam, R. (2024). Developing gene therapy for mitigating multisystemic pathology in Fabry disease: proof of concept in an aggravated mouse model. Hum. Gene Ther. *35*, 680–694.

37. Willer, T., Hordeaux, J., Tsai, P.-C., Ellsworth, D., Mehta, N., Eisenach, H., Shen, J., Louboutin, J.-P., Yu, H., Bell, P., et al. (2021). Development of a novel gene therapy

for Fabry disease: engineered alpha-galactosidase A transgene for improved stability [poster]. Presented at. Annual WORLDSymposium.

38. Hallows, W.C., Skvorak, K., Agard, N., Kruse, N., Zhang, X., Zhu, Y., Botham, R.C., Chng, C., Shukla, C., Lao, J., et al. (2023). Optimizing human α-galactosidase for treatment of Fabry disease. Sci. Rep. *13*, 4748.

39. Jeyakumar, J.M., Kia, A., Tam, L.C.S., McIntosh, J., Spiewak, J., Mills, K., Heywood, W., Chisari, E., Castaldo, N., Verhoef, D., et al. (2023). Preclinical evaluation of FLT190, a liver-directed AAV gene therapy for Fabry disease. Gene Ther. *30*, 487–502.

40. Yasuda, M., Huston, M.W., Pagant, S., Gan, L., St Martin, S., Sproul, S., Richards, D., Ballaron, S., Hettini, K., Ledeboer, A., et al. (2020). AAV2/6 gene therapy in a murine model of Fabry disease results in supraphysiological enzyme activity and effective substrate reduction. Mol. Ther. Methods Clin. Dev. *18*, 607–619.

41. Hughes, D.A. (2022). Safety and efficacy of FLT190 for the treatment of patients with Fabry disease: results from the MARVEL-1 phase 1/2 clinical trial [oral presentation]. Presented at. Annual WORLDSymposium.

42. Hopkin, R.J. (2024). Isaralgagenecivaparvovec(ST-920) gene therapy in adults with Fabry disease: Updated results from an ongoing Phase 1/2 study (STAAR) [oral presentation]. Presented at. Annual WORLDSymposium.

43. Park, J., Murray, G.J., Limaye, A., Quirk, J.M., Gelderman, M.P., Brady, R.O., and Qasba, P. (2003). Long-term correction of globotriaosylceramide storage in Fabry mice by recombinant adeno-associated virus-mediated gene transfer. Proc. Natl. Acad. Sci. USA *100*, 3450–3454.

44. Takahashi, H., Hirai, Y., Migita, M., Seino, Y., Fukuda, Y., Sakuraba, H., Kase, R., Kobayashi, T., Hashimoto, Y., and Shimada, T. (2002). Long-term systemic therapy of Fabry disease in a knockout mouse by adeno-associated virus-mediated muscle-directed gene transfer. Proc. Natl. Acad. Sci. USA *99*, 13777–13782.

45. Namer, B., Ørstavik, K., Schmidt, R., Mair, N., Kleggetveit, I.P., Zeidler, M., Martha, T., Jorum, E., Schmelz, M., Kalpachidou, T., et al. (2017). Changes in ionic conductance signature of nociceptive neurons underlying Fabry disease phenotype. Front. Neurol. *8*, 335.

46. Üçeyler, N., Biko, L., Hose, D., Hofmann, L., and Sommer, C. (2016). Comprehensive and differential long-term characterization of the alpha-galactosidase A deficient mouse model of Fabry disease focusing on the sensory system and pain development. Mol. Pain *12*, 1744806916646379.

47. Ohshima, T., Schiffmann, R., Murray, G.J., Kopp, J., Quirk, J.M., Stahl, S., Chan, C.C., Zerfas, P., Tao-Cheng, J.H., Ward, J.M., et al. (1999). Aging accentuates and bone marrow transplantation ameliorates metabolic defects in Fabry disease mice. Proc. Natl. Acad. Sci. USA *96*, 6423–6427.

48. Ashe, K.M., Budman, E., Bangari, D.S., Siegel, C.S., Nietupski, J.B., Wang, B., Desnick, R.J., Scheule, R.K., Leonard, J.P., Cheng, S.H., and Marshall, J. (2015). Efficacy of enzyme and substrate reduction therapy with a novel antagonist of glucosylceramide synthase for Fabry disease. Mol. Med. *21*, 389–399.

49. Marshall, J., Ashe, K.M., Bangari, D., McEachern, K., Chuang, W.L., Pacheco, J., Copeland, D.P., Desnick, R.J., Shayman, J.A., Scheule, R.K., and Cheng, S.H. (2010). Substrate reduction augments the efficacy of enzyme therapy in a mouse model of Fabry disease. PLoS One *5*, e15033.

50. Mirzaian, M., Wisse, P., Ferraz, M.J., Marques, A.R.A., Gaspar, P., Oussoren, S.V., Kytidou, K., Codée, J.D.C., van der Marel, G., Overkleeft, H.S., and Aerts, J.M. (2017). Simultaneous quantitation of sphingoid bases by UPLC-ESI-MS/MS with identical (13)C-encoded internal standards. Clin. Chim. Acta *466*, 178–184.